

SPIRAL CREEPING WAVES IN ULTRASONIC ANGLED-BEAM SHEAR WAVE INSPECTION OF FASTENER HOLES IN MULTILAYER STRUCTURES

John C. Aldrin¹, Jeremy Knopp², Dave Judd³, John R. Mandeville³, Eric Lindgren³,

¹Computational Tools, Gurnee, IL 60031, USA

²Air Force Research Laboratory (AFRL/MLLP), Wright-Patterson AFB, OH 45433, USA

³SAIC Ultra Image Int., New London, CT 06320, USA

Abstract. This paper explores the propagation and scattering of spiral creeping waves around a fastener hole. Preliminary experimental data demonstrates the presence of spiral creeping waves in angled beam inspection and the benefit for detecting cracks of varying angular location. Analytical models are used to provide insight into the propagation and focusing of spiral creeping waves around cylindrical holes. A hybrid numerical method is proposed as a measurement model for 3D scattering from holes with cracks.

Keywords: cracks, cylindrical holes, modeling, spiral creeping wave, ultrasonics

PACS: 81.70.Cv

INTRODUCTION

Due to the potential for catastrophic failure, fatigue cracks in aircraft structures are of significant concern. Given inherent stress concentrations, fastener holes in aircraft structures are primary locations for crack initiation. The early detection of cracks at maintenance intervals is necessary to maintain safety and minimize repair cost. Thus, a general goal of structural engineers is to find and characterize flaws while they are still sufficiently small that they can be repaired with minimal cost and limited interruption to the availability of the aircraft. The inspection of aircraft holes that contain fasteners with small fatigue cracks has a long history in NDE, given the complexity of the inspection problem. The bolt hole eddy current technique has the capability to detect small cracks, but requires the removal of the fastener. Ultrasonic angle-beam shear wave inspections have been developed to address crack detection in multilayer structures without fastener removal. Early work to develop a wide-area automated ultrasonic technique for corrosion detection in the DC-9 wing box laid the foundation for future applications using angle-beam shear waves [1]. An inspection procedure for the detection of cracks around fasteners in the C-141 spanwise splice joint was developed incorporating automated scanning and imaging, validated through a probability of detection (POD) study, and implemented for regular depot maintenance [1]. A recent development program for the C-130 hat section holes included automated defect analysis (ADA) software and an on-wing immersion system (ACES) which was also validated through a successful POD study [2]. However for these applications, full 360° coverage around the hole was not required based a priori knowledge of the loading conditions and failure mode.

For inspection problems requiring full 360° coverage, several approaches have been investigated using ultrasonic angled-beam shear wave techniques. Mechanically

configurations for rotating an ultrasonic transducer around a fastener site have been successfully applied [3], but they are time intensive requiring accurate positioning and mechanical operation. Ultrasonic phased array transducers incorporating 504 elements have also been developed to scan 360° electronically, but also require manual centering of the probe [4]. Lastly, linear phased arrays with single axis linear scanners have been used to improve scan coverage versus 2D raster scan approaches [5]. However, the proposed approach requires six separate scans for each head position to ensure full 360° coverage.

To supplement traditional mechanisms of crack detection based on corner reflection and crack tip diffraction, the concept of generating and detecting ‘spiral’ creeping waves is presented. A diagram of this concept is presented in Figure 1. The use of creeping waves for the inspection of cracks around holes in vertical riser structures has been explored for empty (weep) holes [6], holes with coatings or holes filled with fluid [7], and holes containing fastener wet installed with sealant [8,9]. As shown in Figure 1, a spiral creeping wave is generated by an incident shear wave on a curved hole surface, which propagates in a spiral direction and interacts with cracks in the shadow region of the hole. Due to the curvature of the hole, any reflected spiral creeping wave from a crack leaks away from the hole and can be measured in either pulse-echo or pitch-catch modes. Potential benefits of the approach include greater sensitivity to cracks of varying angular location, and improved sensitivity to skewed cracks where the crack is not perpendicular to the hole. In addition, this approach is expected to reduce inspection time, given the potential to eliminate the need for multiple scans with varying head position (for linear scans) and single hole centering (for circumferential scans).

To best apply this approach to the inspection problem of fastener holes in layered horizontal structures, a better understanding of the physics is needed for complex 3D ultrasonic scattering problems incorporating guided waves on curved surfaces with radial fatigue cracks. First, experimental data is used to demonstrate the presence of spiral creeping waves in angled beam inspection and also emphasize the benefit in detecting cracks of varying angular location. Analytical models are also used to provide insight into the propagation and focusing of spiral creeping waves around cylindrical holes. Lastly, hybrid numerical methods are proposed as measurement models for 3D scattering from holes with cracks. With this understanding, the ability to improve the design of ultrasonic array transducers for fastener hole inspection and improve the design of data analysis algorithms is expected.

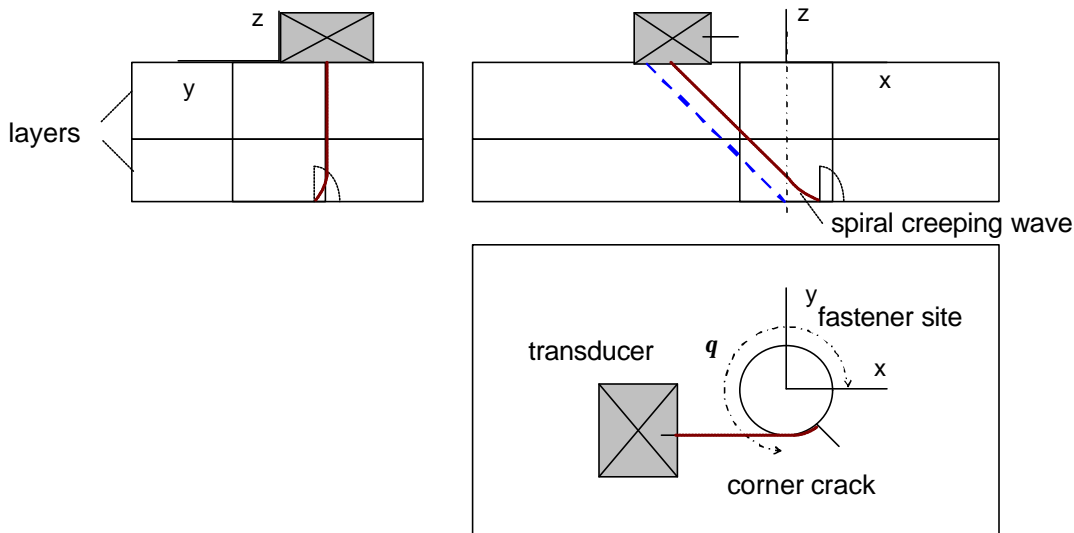


FIGURE 1. Schematic diagram of the ultrasonic inspection of fastener sites for corner cracks in multilayer structures using spiral creeping waves to detect corner cracks in the shadow region of the hole.

EXPERIMENTAL STUDY

To explore the influence of spiral creeping waves on an ultrasonic angled-beam shear wave inspection technique, a study was performed varying the angular location of the flaw. A series of C-scan images were acquired according to the C-130 hat section hole inspection procedure [7]. The scan increments were 0.020" in both the x and y directions. The samples used for the study contained 0.070" EDM corner notches in the second layer in both the 'above hole' and 'below hole' crack (notch) positions. Of particular interest is the below hole position where the notch is incrementally rotated away from the transducer into the shadow region of the hole.

C-scan images with schematic diagrams are shown in Figure 2 for four EDM corner notch angular locations, (a) $q = 0^\circ$, (b) $q = 10^\circ$, (c) $q = 20^\circ$, (d) $q = 40^\circ$. At the center of each image is the characteristic fastener site feature resulting from a superposition of multiple specular reflections from the bottom and top corners of the hole in each panel layer. Both upper and lower EDM notch features can be observed as characteristic 'mouse ears' located to the right and above / below the hole feature. For $q = 0^\circ$, the lower feature begins with a strong wide feature associated with the presence of a notch. As the crack location is shifted from $q = 0^\circ$ to $q = 10^\circ$, the crack feature begins to distort with a small second peak shifted in the y and x directions. (Note, for a path of 0.500" in the x direction, the change in the y direction due to a 10° crack shift would be 0.087", which corresponds to 4 pixels in the image.) As the angle is further shifted, such as at $q = 40^\circ$, very little corner reflection from the root of the notch with the bottom of the panel is expected to be measured, however, signals of significant magnitude can still be found. This feature also narrows, potentially indicating a sensitivity concerning the transducer position and the generation of the spiral creeping wave. Although the notch features are primarily attributed to corner reflection of the incident shear wave, preliminary experimental data demonstrates the existence of the 'spiral' creeping waves in angled beam inspection.

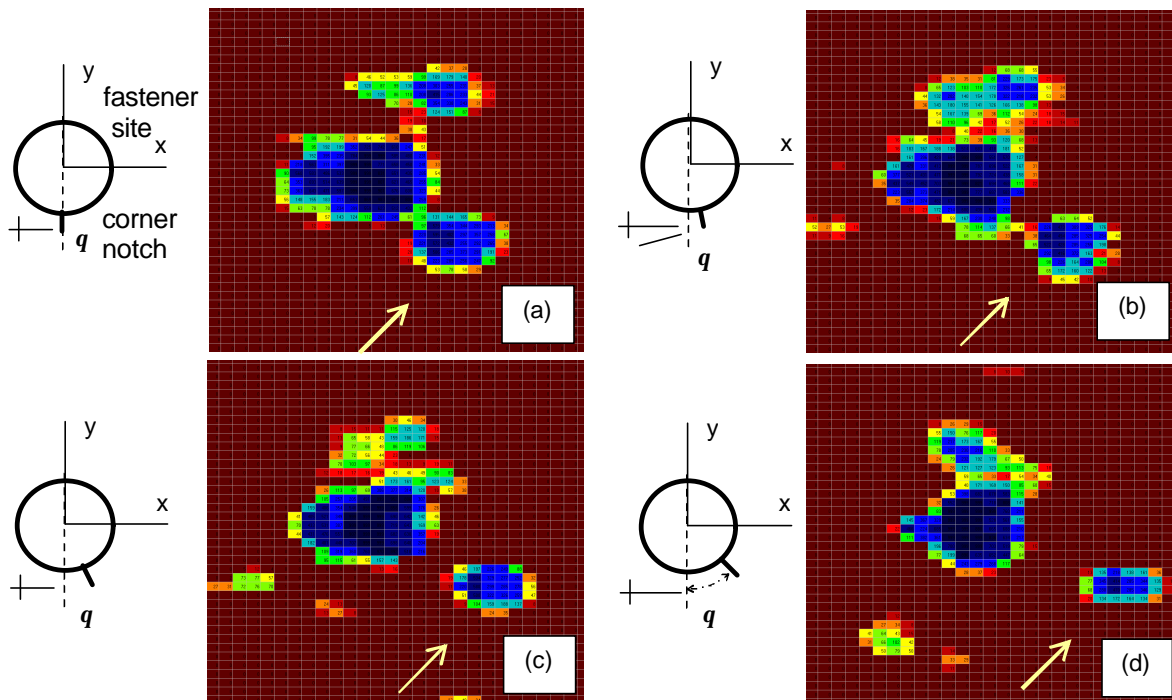


FIGURE 2. C-scan images with diagrams of the C-130 hat section holes with 2nd layer far (below hole) and near (above hole) 0.070" EDM corner notches of varying angular location: (a) 0°, (b) 10°, (c) 20°, (d) 40°.

RAY THEORY ANALYSIS OF SPIRAL CREEPING WAVE

To initially explore the path characteristics and wave speed of a spiral creeping wave as it propagates around a cylindrical hole, an analytical model using ray theory is presented. In particular, the path of a spiral creeping wave generated by an incident shear wave will be investigated as shown in Figure 3(a). A parametric equation model can be used to represent the path of the spiral creeping wave such that

$$x = r \cos(\mathbf{w}_{xy} t'), \quad (1)$$

$$y = r \sin(\mathbf{w}_{xy} t'), \quad (2)$$

$$z = t', \quad (3)$$

where t' and \mathbf{w}_{xy} represent time and frequency parameters respectively. In Figure 3(b), the distance traveled along the path length, ds , can be expressed in terms of the angle of incidence, \mathbf{j} , and the change in the vertical location along the path, dz ,

$$ds = dz [\sin(\mathbf{j})]^{-1}. \quad (4)$$

The distance traveled along the path can also be expressed in terms of the change in time of flight, dt , and the phase velocity of the spiral creeping wave, c_p ,

$$ds = c_p dt. \quad (5)$$

Thus, the time and frequency parameters, and the parametric path variables respectively can be rewritten as a function of the angle of incidence and phase velocity

$$dt' = c_p \sin(\mathbf{j}) dt, \quad (6)$$

$$\mathbf{w}_{xy} = \frac{1}{r} \cot(\mathbf{j}), \quad (7)$$

$$x(t) = r \cos \left[\frac{c_p}{r} \cos(\mathbf{j}) t \right], \quad (8)$$

$$y(t) = r \sin \left[\frac{c_p}{r} \cos(\mathbf{j}) t \right], \quad (9)$$

$$z(t) = c_p \sin(\mathbf{j}) t. \quad (10)$$

To evaluate the phase velocity of the spiral creeping wave, an approximation is made using the 2D analytical solution for waves propagating along a concave cylindrical surface [10]. Locally, the radius of curvature of the spiral path is defined by an ellipse as a cut through the cylinder in the direction of propagation as shown in Figure 3(a) and 3(c). For the ellipse, the dimensions along the minor and major axes in terms of the incident angle are given by:

$$a = r / \cos(\mathbf{j}), \quad (11)$$

$$b = r. \quad (12)$$

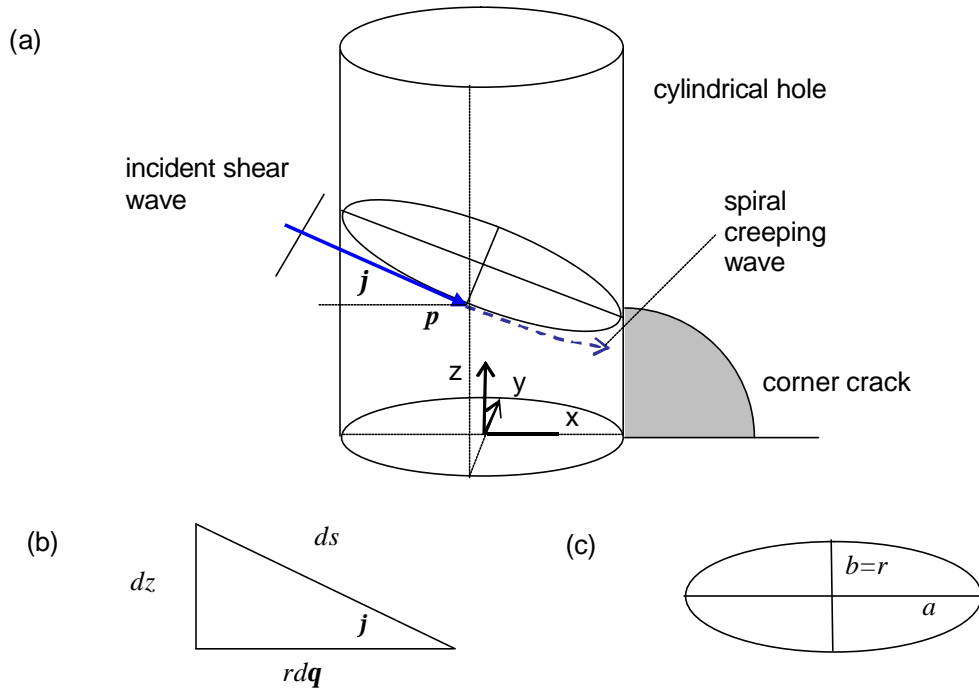


FIGURE 3. (a) Diagram of plane cut by an incident wave at a point on a cylinder with (b) cross-section showing relation between the incident angle and path length and (c) dimensions of the ellipse.

Thus, the local radius of curvature for the spiral creeping wave, associated with the minor axis of the ellipse, is given by

$$R = a^2/b = r/[\cos(\mathbf{j})]^2. \quad (13)$$

Viktorov previously studied the sensitivity of phase velocity and attenuation to variation in the product of the wavenumber, k_R , and the radius of curvature [10]. This solution can be obtained by deriving the frequency equation given by

$$\left[2 - b^2 - \frac{2}{n}(aHA^{(1)} - 1)\right] \left[2 - b^2 - \frac{2}{n}(bHB^{(1)} - 1)\right] - 4 \left[aHA^{(1)} - 1 - \frac{1}{n}\right] \left[bHB^{(1)} - 1 - \frac{1}{n}\right] = 0, \quad (14)$$

$$\text{with: } n = ka, k = \frac{w}{c}, \mathbf{a} = \frac{c}{c_L}, \mathbf{b} = \frac{c}{c_T}, HA^{(1)} = \frac{H_{n-1}^{(1)}(\mathbf{a}ka)}{H_n^{(1)}(\mathbf{a}ka)}, HB^{(1)} = \frac{H_{n-1}^{(1)}(\mathbf{b}ka)}{H_n^{(1)}(\mathbf{b}ka)},$$

where c ($= c_p$) is the wave speed of the spiral creeping wave, c_L is the longitudinal wave speed, c_T is the transverse wave speed, and a is the radius of hole. In order to solve this equation for the complex angular wavenumber, n , an iterative search routine for the complex solution space is required. Viktorov also derived an approximate explicit solution of the form [10]:

$$c_p = c_R(1 - \mathbf{d}) = c_R \left(1 - \frac{A(c_L, c_T)}{k_R R}\right). \quad (15)$$

The product of the wavenumber and the radius of curvature can be rewritten in terms of the incident angle, radius of the hole, Rayleigh wave phase velocity, and frequency

$$k_R R = \frac{2pfa}{c_R} [\cos(\mathbf{j})]^{-2}. \quad (16)$$

Thus, the phase velocity of the spiral creeping wave can be approximated using the following relation

$$c_p = c_R \left(1 - \frac{A(c_L, c_T) c_R}{2pfa} [\cos(\mathbf{j})]^2 \right). \quad (17)$$

Figure 4 present a plot of the normalized phase velocity of the spiral creeping wave (with respect to the Rayleigh wave phase velocity) as a function of incident angle. For this study, the following model properties were used: $c_L = 6301$ m/s, $c_T = 3103$ m/s, $c_R = 2897$ m/s, $a = 2.38$ mm (3/16"), $f = 5.0$ MHz, and $k_R R = 25.8$. For \mathbf{j} approaching 90° , the local curvature becomes flat and thus the phase velocity approaches the solution for a Rayleigh wave propagating on a half-space. As \mathbf{j} is reduced from 90° to 0° , the phase velocity is reduced to a minimum of about 92 - 93% of the Rayleigh wave velocity. Thus, some consideration must be given to the selection of the transducer frequency and beam incident angle for a given radius to optimize a spiral creeping wave signal to scatter from a radial crack.

Figure 5 presents a plot of a series of spiral creeping wave paths for \mathbf{j} from 0° to 85° at increments of 5° degrees. Also shown are a series of (dashed blue) lines of constant time of flight. This study provides insight into the problem of focusing rays to a particular point of interest about the cylinder. As the angle of incidence is decreased, the wave speed decreases; however, the travel path is shorter. Conversely, as the angle of incidence is increased the wave speed increases but the travel path to the point of interest also increases. Array transducers may provide a significant advantage toward improving the focusing capability of spiral creeping waves on a cylindrical surface. Selection of transducer position, beam orientation and profile, and time delays are important factors when considering the optimizing the generation and detection of spiral creeping waves.

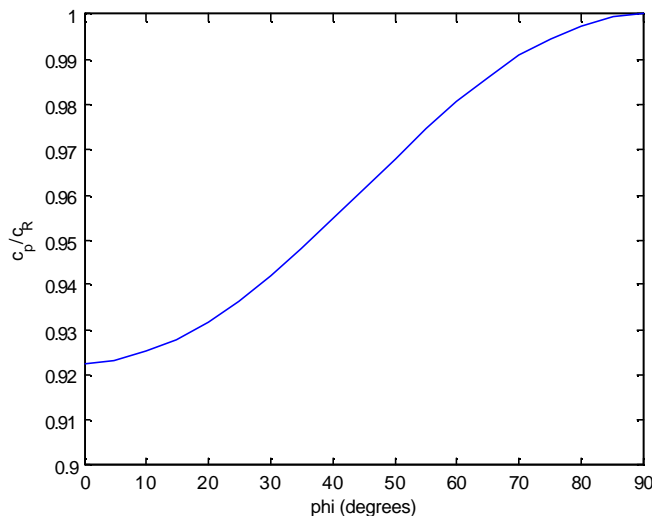


FIGURE 4. Plot of spiral creeping wave phase velocity as a function of angle of incidence.

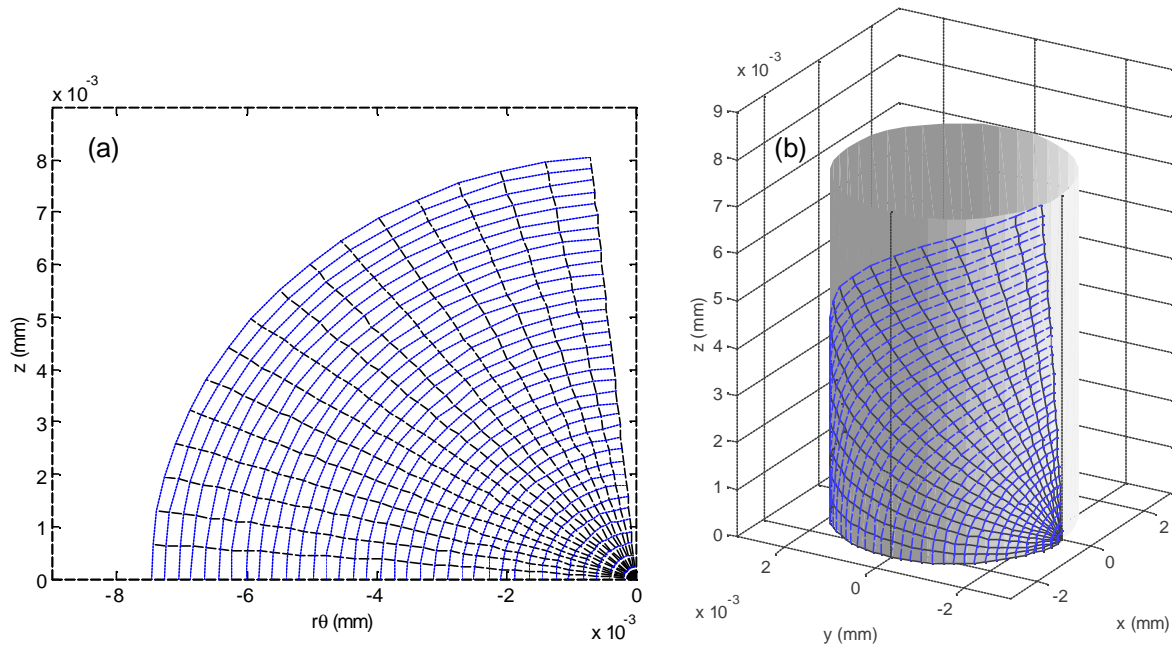


FIGURE 5. Plot of rays of propagating spiral creeping waves (solid black) for increments of \mathbf{j} every 5° with lines of constant time of flight (dashed blue) in (a) 2D and (b) 3D.

NUMERICAL MODELING APPROACH FOR 3D ULTRASONIC SCATTERING PROBLEM

Preliminary analysis based on analytical models has provided some insight into the nature of spiral creeping waves as they propagate around a cylindrical hole; however, 3D models will be essential to study the physics of this complex ultrasonic scattering problem. Guided wave techniques have been proposed to find small flaws around fasteners in thin aircraft structures. To study these problems, finite element and finite difference methods have been successfully applied to model guided wave scattering from holes with fatigue cracks [11]. However, these computational methods have mostly been applied to relatively thin structures. Unfortunately, fast 3D simulations for the scattering of guided waves such as the spiral creeping wave from cracks around fastener sites are not available.

A significant area of research is the development of efficient 3D simulations for this class of ultrasonic scattering problem. Hybrid approaches have been investigated in order to save considerable computational time for such problems. Of particular promise is a hybrid approach using semi-analytical transducer models with 3D explicit FEM modeling to solve the localize scattering problem [12]. This approach provides accurate measurement models that would address the complexity, speed, and memory requirements for these 3D problem. To minimize development time and cost for the hybrid numerical model, the integration of existing transducer models and FEM software was performed. The low cost, open source FEM package, FEAP, was used to solve the local 3D explicit finite element method problem [13]. Integration with Matlab was facilitated using FEAPMEX, providing integration with existing transducer models and visualization tools. Perfectly matched layers were also implemented as absorbing boundary conditions to help reduce the size of the meshed domain and thus minimize solution time.

To date, validation studies have been performed in 2D using accurate transducer models and in 3D using only point source excitation. Future work will explore the generation and scattering of spiral creeping waves around a fastener site with corner fatigue cracks using both visualization and measurement models.

CONCLUSIONS AND FUTURE WORK

Preliminary experimental data demonstrates the presence of spiral creeping waves in angled beam inspection and the benefit for detecting cracks of varying angular location. Analytical models are used to provide insight into the propagation and focusing of spiral creeping waves around cylindrical holes. Also, a hybrid numerical model is presented to study scattering of spiral creeping waves from cracks around fasteners. Benefits of the effort include a fundamental understanding of the ultrasonic scattering phenomena, aid in design of ultrasonic methods to minimize inspection time, and the capability to better locate and characterize flaws around fastener sites using ultrasonic NDE transducers and potentially in aircraft structures using in situ sensors. Future parametric experimental studies are planned to investigate sensitivity of spiral creeping waves to flaw location and size, hole condition, and transducer characteristics. Using the numerical model, simulated studies are planned to explore transducer design and the fastener hole interface condition.

ACKNOWLEDGEMENTS

Funding was provided by the Air Force Office of Scientific Research through AFRL/MLLP, Wright Patterson AFB OH.

REFERENCES

1. Mullis, R. T., and MacInnis, T., "C-141 Spanwise Splice Advanced NDI Method", First Joint DoD/FAA/NASA Conference on Aging Aircraft, Ogden, Utah, (July 8-10, 1997).
2. Lindgren, E., et al., "Validation and Deployment of Automated Ultrasonic Inspections for the C-130 Center Wing", ASIP Conference, Savannah, Georgia, (Dec. 2 - 4, 2003).
3. MacInnis, T., et al., "New Ultrasonic Based Multi-Layer Inspection Technique for the B-1B Aircraft", 6th Joint DoD/FAA/NASA Conf. on Aging Aircraft, (Sept. 16-19, 2002).
4. Moles, M., et al., "FastFocus Phased Array System for Air Plane Fastener Inspections", 16th World Conference on Nondestructive Testing, Montreal, Canada, (2004).
5. Smith et al., "Rapid second-layer crack detection using phased-arrays and automated analysis", Aging Aircraft Conf., Palm Springs, California, (Jan 31 – Feb. 3, 2005).
6. P.B. Nagy, M. Blodgett, M. Golis, "Weep hole Inspection by Circumferential Creeping Waves" *NDT&E International*, **27**, 131 (1994).
7. Aldrin, J., Achenbach, J. D., "Models for Crack Detection in a Cylindrical Hole Containing an Elastic Layer and a Fluid-Filled Cylindrical Hole," *Rev Prog Quant Nondestr Eval*, **22**, 181-189, (2003).
8. Aldrin, J. C., Mandeville, J. R., Kropas-Hughes, C. V., "Ultrasonic Detection of Cracks in a Complex Aircraft Structure Using a Local Correlation Method for Signals from a Moving Transducer", *Rev Prog Quant Nondestr Eval*, **23**, 565-572, (2004).
9. Lindgren, E., et al., "Validation and Deployment of Automated Ultrasonic Inspections for the C-130 Center Wing," ASIP Conference, Savannah, Georgia, (Dec. 2 – 4, 2004).
10. Viktorov, I.A., *Rayleigh and Lamb waves* (Plenum Press, New York, 1967).
11. Fromme, P., Sayir, M. B., "Monitoring of fatigue crack growth at fastener holes using guided Lamb waves," *Rev Prog Quant Nondestr Eval*, **21**, 247-254, (2002).
12. Gengembre, N., Lhemery, A., Omote, R., Fouguet, T., Schumm, A., "A semi-analytical-FEM hybrid model for simulating UT configurations involving complicated interactions of waves with defects," *Rev Prog Quant Nondestr Eval*, **23**, 74-80, (2004).
13. Taylor, R. L., *FEAP - A Finite Element Analysis Program, Theory Manual*, University of California, Berkeley, <http://www.ce.berkeley.edu/~rlt>.